



Study of Jet Substructure Variables for the Future Detector

*Chih-Hsiang Yeh¹, Shin-Shan Eiko YU¹, Ashutosh Kotwal^{2,3},
Sergei Chekanov⁴, Nhan Viet Tran³



¹Department of Physics, National Central University, Chung-Li, Taoyuan City 32001, Taiwan

²Physics, Duke University, Durham, NC 27708, USA

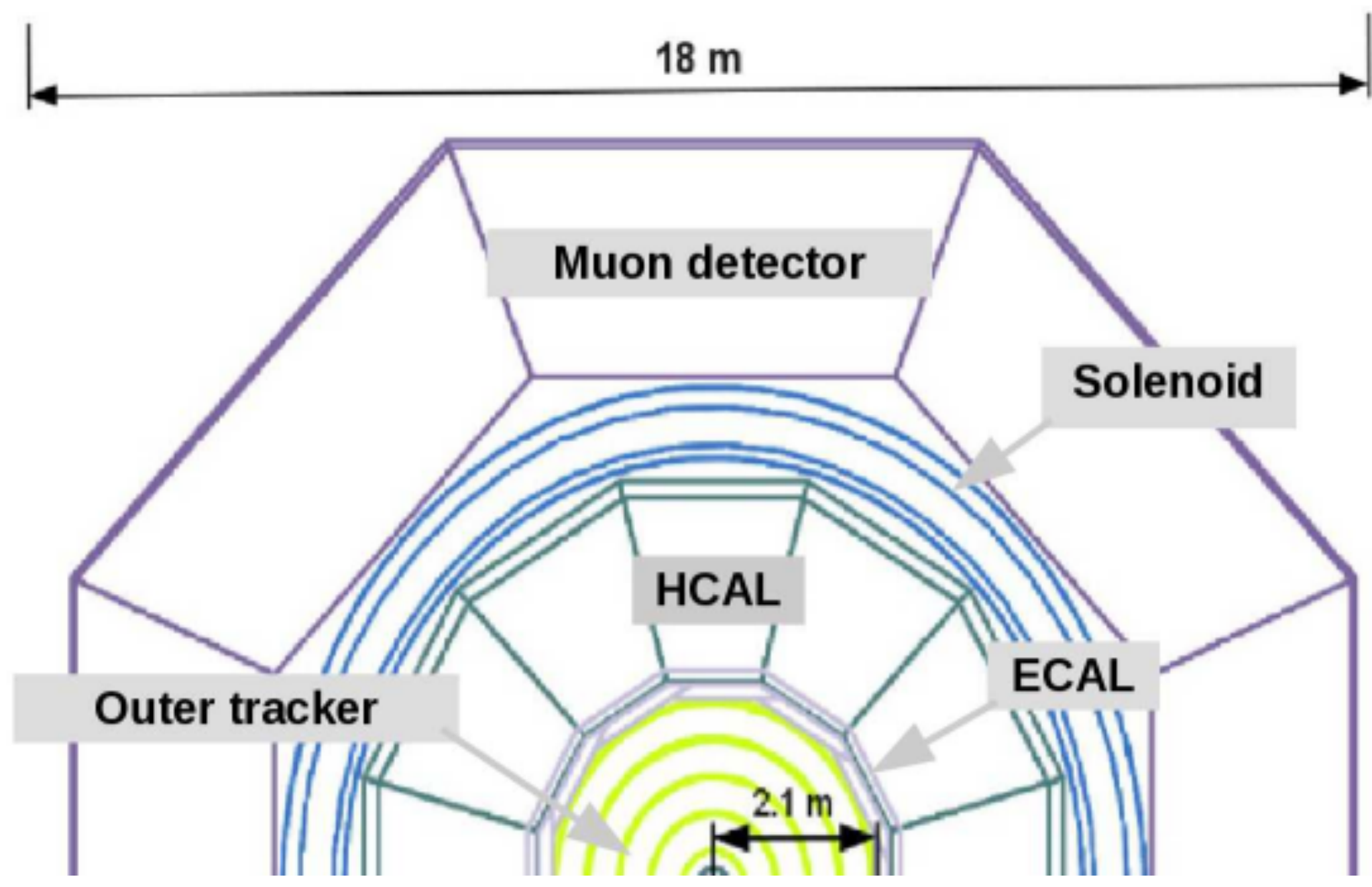
³Fermi National Accelerator Laboratory, Batavia, IL 6051, USA

⁴HEP Division, Argonne National Laboratory, 9700 S. Cass Avenue, Argonne, IL 60439, USA

Abstract:

In this poster, we study the performance of hadron calorimeter in SiFCC for the future $\sqrt{s}=100$ TeV pp collider. The GEANT4 full simulation includes calorimeters with different cell sizes. We aim to efficiently separate signal $Z' \rightarrow WW$ or $Z' \rightarrow tt$ and background $Z' \rightarrow qq$. Various jet substructure variables and Z' masses from 5 to 40 TeV are also compared.

Geant 4 Simulation of Future Detector SiFCC



Barrel	Technology	pitch/cell	radii (cm)	$ z $ size (cm)
Vertex detector	silicon pixels/5 layers	25 μm	1.3 - 6.3	38
Outer tracker	silicon strips/5 layers	50 μm	39 - 209	921
ECAL	silicon pixels+W	2x2 cm	210 - 230	976
HCAL	scintillator+steel	5x5 cm	230 - 470	980
Solenoid	5 T (inner), -0.6 T (outer)	-	480 - 560	976
Muon detector	RPC+steel	3x3 cm	570 - 903	1400

Basic Jet Reconstruction Algorithm:

$$d_{ij} = \min(k_{ti}^2 p, k_{tj}^2 p) \frac{\Delta_{ij}^2}{R^2}$$

$$\Delta_{ij}^2 = (y_i - y_j)^2 + (\phi_i - \phi_j)^2$$

i, j : the i and j particle
 k_{ti}, k_{tj} : the particle i and j transverse momentum

If $d_{ij} < d_{ib}$, j particle will be merged in I particle

- 1.p=0 : Cambridge/Aachen algorithm
- 2.p=1 : kt algorithm
- 3.p=-1 : anti-kt algorithm

Jet Substructure Variables:

1.N-subjetness:

$$\tau_N = \frac{1}{d_0} \sum_k P_{t,k} \min\{\Delta R_{1,k}, \Delta R_{2,k}, \dots, \Delta R_{N,k}\}$$

$$d_0 = \sum_k P_{t,k} R_0$$

$\Delta R_{i,k}$: The distance between constituent in the eta - phi plane

R_0 : The cone size we want to cluster

$$\tau_{21} = \frac{\tau_2}{\tau_1}, \tau_{32} = \frac{\tau_3}{\tau_2}$$

2.Energy correlation function:

$$ECF(N, \beta) = \sum_{i_1 < i_2 < \dots < i_N \in J} \left(\prod_{a=1}^N P_{T,ia} \right) \left(\prod_{b=1}^{N-1} \prod_{c=b+1}^N \Delta R_{ibic} \right)^\beta$$

$$C_N^{(\beta)} \equiv \frac{ECF(N+1, \beta) ECF(N-1, \beta)}{ECF(N, \beta)^2}$$

3.Soft drop:

$$\frac{\min(P_{T1}, P_{T2})}{P_{T1} + P_{T2}} < Z_{cut} \left(\frac{\Delta R_{12}}{R_0} \right)^\beta$$

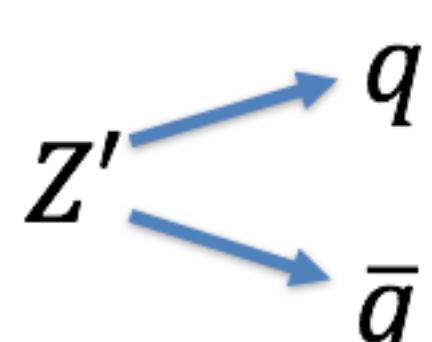
$\beta > 0$: Remove (soft), maintain (soft - collinear)

$\beta = 0$: Depend on the cut to select the asymmetry

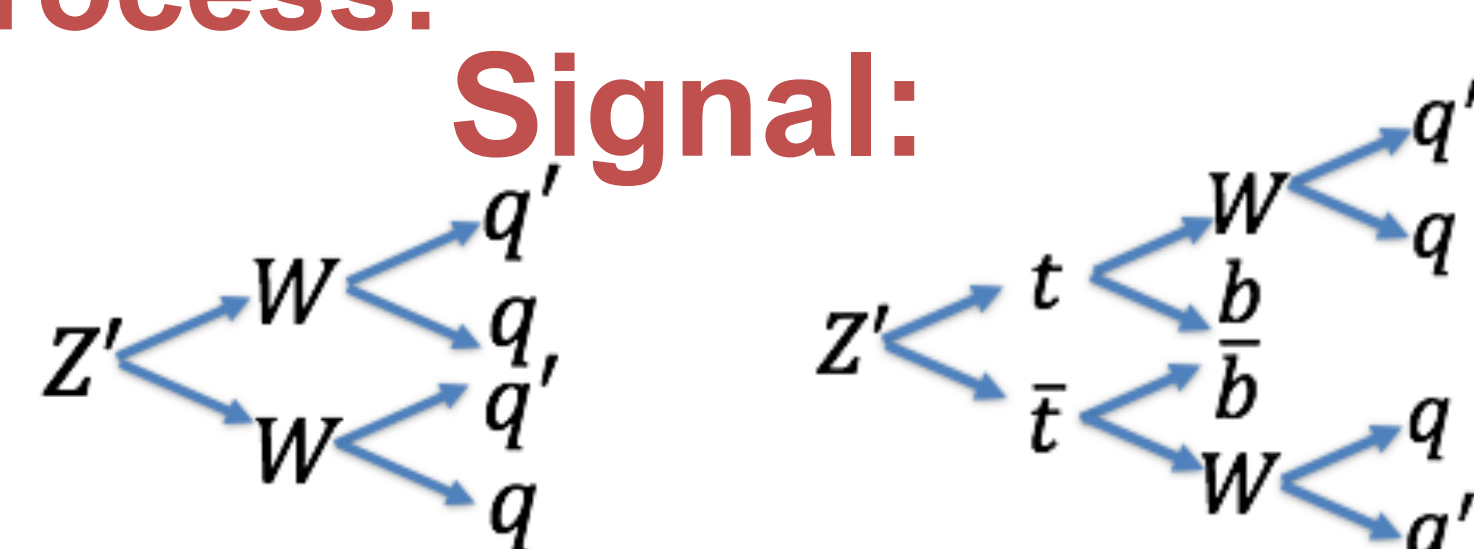
$\beta < 0$: Remove both (soft) and (collinear)

Signal and Background Process:

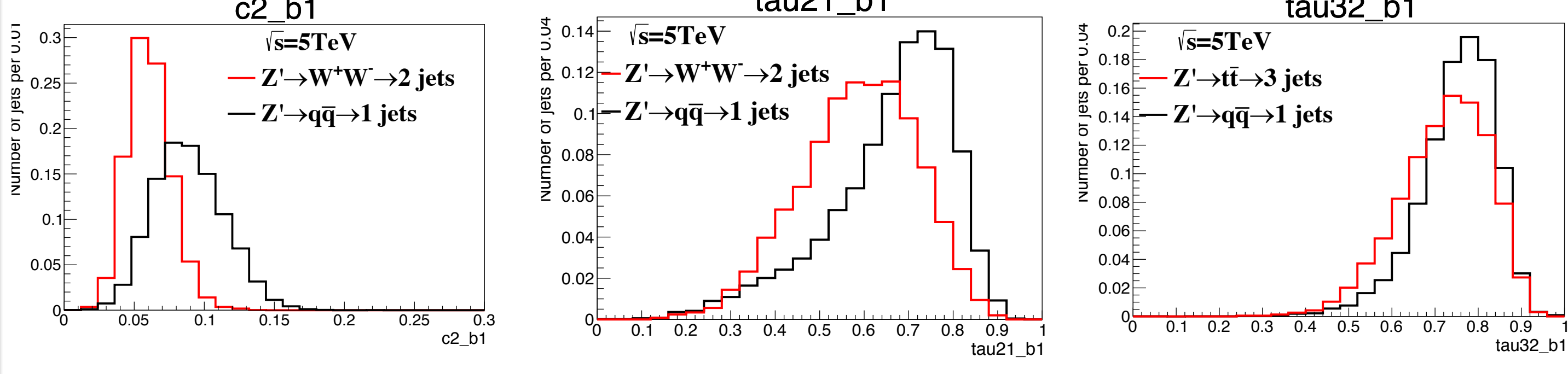
Background:



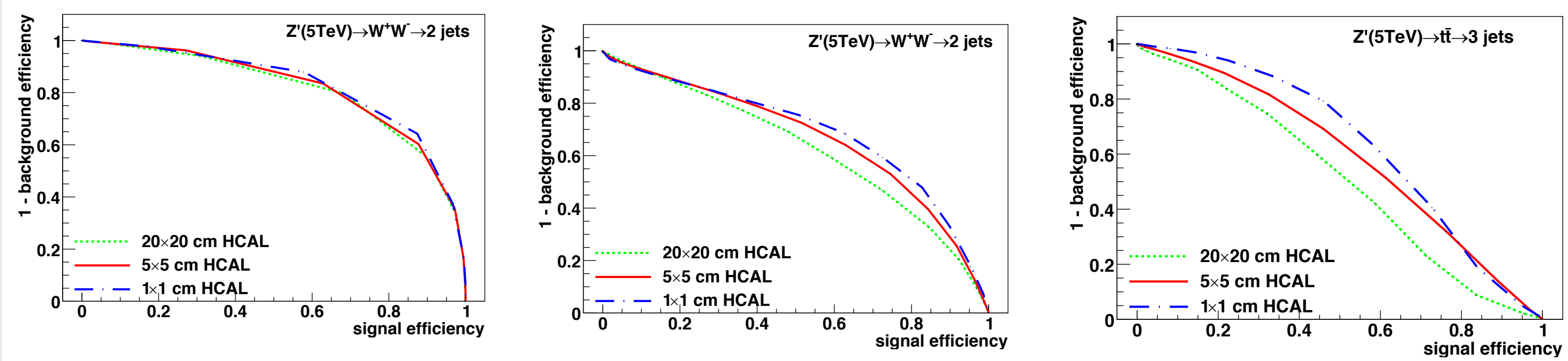
Signal:



Variables Study in $C_2^1, \tau_{21}, \tau_{32}$: Distribution of $z' \rightarrow WW, z' \rightarrow qq$ and $z' \rightarrow tt, z' \rightarrow qq$:



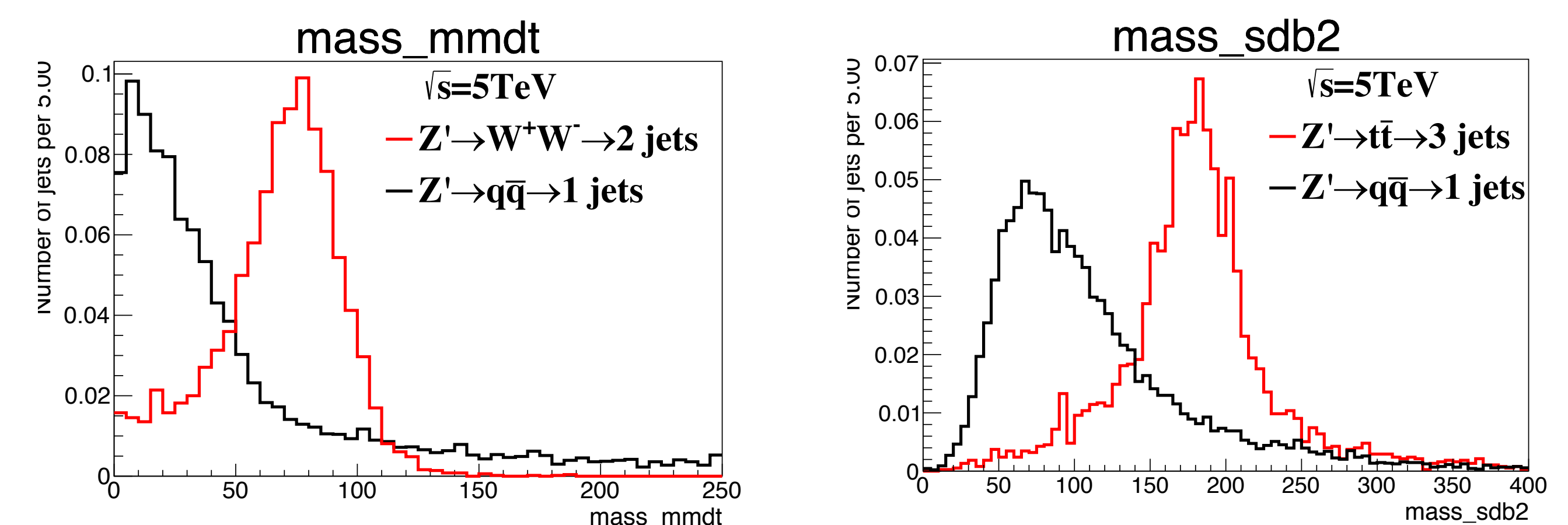
Comparison of different detector size:



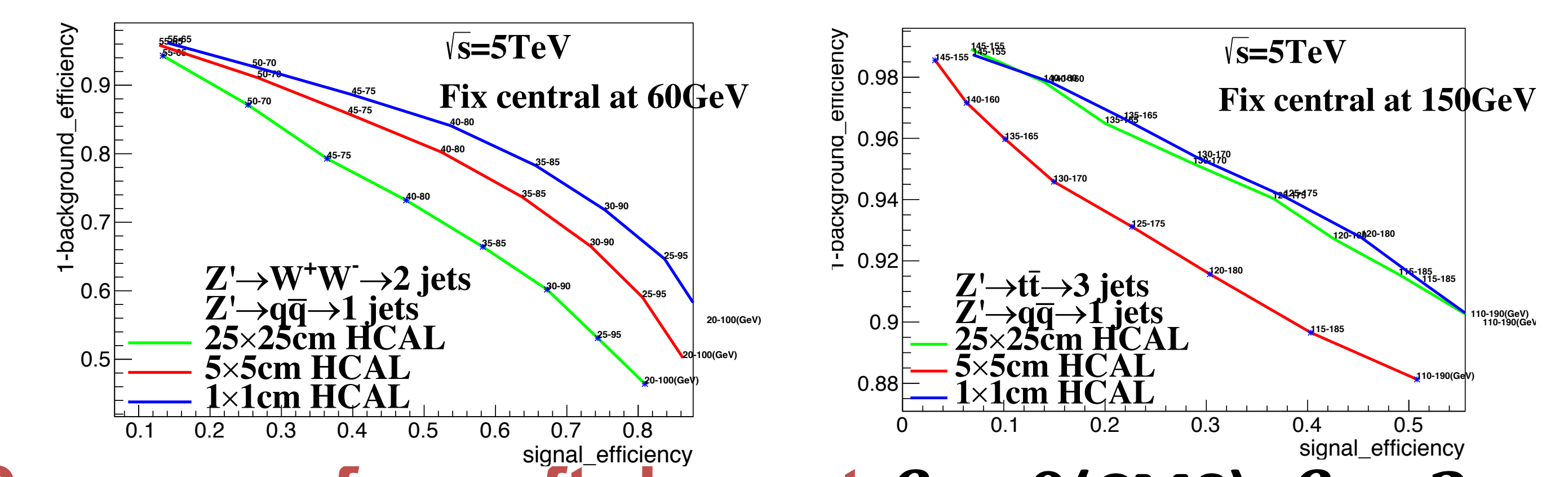
Summary for $C_2^1, \tau_{21}, \tau_{32}$:

1. For C_2^1 , the ROC curves of the three detector cell sizes are close to each other for each collision energy. Therefore, this variable is not sensitive to the detector cell size.
2. For τ_{21} , at 5 TeV, the smallest detector size can separate the background from the signal well. However, this is not the usual case as the ROC curves nearly merge together at higher collision energy.
3. For τ_{32} , the smallest detector size has the best separation power for all collision energies.

Study of Soft Drop at $\beta = 0$ (CMS), $\beta = 2$:



Comparison of different detector size:



Summary for soft drop at $\beta = 0$ (CMS), $\beta = 2$:

Is it the best for smallest detector size?

Fix central (from near highest)	$\sqrt{s} = 5\text{TeV}$	$\sqrt{s} = 10\text{TeV}$	$\sqrt{s} = 20\text{TeV}$	$\sqrt{s} = 40\text{TeV}$
$\beta = 0$ Signal=WW	O	O	X	X
$\beta = 2$ Signal=WW	X	X	X	X
$\beta = 0$ Signal=tt	X	O	O	X
$\beta = 2$ Signal=tt	X	X	X	X

Reference :

Initial performance studies of a general-purpose detector for multi-TeV physics at a 100 TeV pp collider(JINST 12 (2017) P06009)